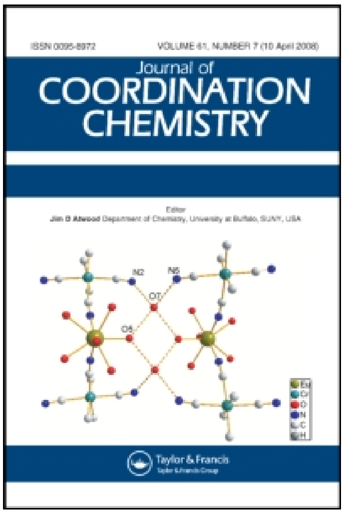

Journal of Coordination Chemistry
Publication details, including instructions for authors and subscription information:
http://www.informaworld.com/smpp/title~content=t713455674

Dinuclear peroxo complexes of molybdenum(VI) containing Mannich base ligands

Rimpy Gupta[a]; Haq Nawaz Sheikh[a]; Mohita Sharma[a]; Bansi Lal Kalsotra[a]
[a] Department of Chemistry, University of Jammu, Jammu-180 006, India

To cite this Article Gupta, Rimpy , Sheikh, Haq Nawaz , Sharma, Mohita and Kalsotra, Bansi Lal(2010) 'Dinuclear peroxo complexes of molybdenum(VI) containing Mannich base ligands', Journal of Coordination Chemistry, 63: 18, 3256 — 3267, First published on: 06 August 2010 (iFirst)

To link to this Article: DOI: 10.1080/00958972.2010.507813

URL: http://dx.doi.org/10.1080/00958972.2010.507813

Journal of Coordination Chemistry
Vol. 63, No. 18, 20 September 2010, 3256–3267

Taylor & Francis
Taylor & Francis Group

Dinuclear peroxo complexes of molybdenum(VI) containing Mannich base ligands

RIMPY GUPTA, HAQ NAWAZ SHEIKH*, MOHITA SHARMA
and BANSI LAL KALSOTRA

Department of Chemistry, University of Jammu, Jammu – 180 006, India

(*Received 19 January 2010; in final form 7 May 2010*)

Dinuclear molybdenum(VI) peroxo complexes containing Mannich base ligands having formulae $[Mo_2O_4(O_2)_2L\text{-}L(H_2O)_2]\cdot H_2O$ [where L-L = N-[1-morpholinobenzyl] acetamide (MBA), N-[1-piperidinobenzyl] acetamide (PBA), N-[1-morpholino(-4-nitrobenzyl)] benzamide (MPNBB), N-[1-piperidino(-3-nitrobenzyl)] benzamide (PMNBB), N-[1-morpholino(-2-nitrobenzyl)] acetamide (MONBA), and N-[1-morpholino(-3-nitrobenzyl)] acetamide (MMNBA)] have been synthesized by stirring ammonium heptamolybdate with excess 30% aqueous hydrogen peroxide followed by treatment with ethanolic solution of corresponding ligands. The complexes have been characterized by elemental analysis, molar conductance, magnetic measurements, infrared (IR), electronic, TGA/DTA, mass spectral, and ^{1}H NMR studies. The complexes are non-electrolytes and diamagnetic. The IR spectral studies suggest that the ligands are bidentate to metal through carbonyl oxygen and ring nitrogen. Thermal analyses provide conclusive evidence for the presence of coordinated, as well as lattice water in the complexes. Dinuclear complexes preserve the individuality of the molybdenum oxo peroxo core. The complexes exhibit higher antibacterial activity against bacterium *Ralastonia solanacearum* (*Pseudomonas solanacearum*) than the free ligands.

Keywords: Mannich base; Peroxo complex; Dinuclear complex; Oxo peroxo core; Antibacterial activity

1. Introduction

Molybdenum possesses many stable and accessible oxidation states. Molybdenum compounds provide active centers for processes, such as hydrosulfurization [1] and oxygen atom transfer reactions, such as olefin epoxidation and de-epoxidation [2]. $[MoO(O_2)_2(OPy)(H_2O)]$ has been shown to be a very effective agent for oxygen-transfer reactions of a wide class of substrates including oxidation of a series of sulfides to sulfoxides [3]. $[MoO(O)_2(C_{10}H_{16}N_4)]$ catalyzes the oxidation of alkyl benzenes in the presence of hydrogen peroxide under atmospheric oxygen in moderate to good yields [4]. Nature has incorporated molybdenum into a number of redox enzymes [2, 5].

Peroxo complexes of molybdenum(VI) have been known for a long time [6, 7] and a variety of peroxo molybdates, coordinated with nitrogen and oxygen donors, have been characterized structurally [8–10] and studied in solution and solid state [11, 12].

---

*Corresponding author. Email: hnsheikh@rediffmail.com

Journal of Coordination Chemistry
ISSN 0095-8972 print/ISSN 1029-0389 online © 2010 Taylor & Francis
DOI: 10.1080/00958972.2010.507813

X-ray data analysis of the mononuclear molybdenum compound $[MoO(O_2)_2(OPy)(H_2O)]$ reveals a pentagonal bipyramidal coordination polyhedron for Mo [3]. The pyridine *N*-oxide (OPy) ligand occupies the equatorial position, with the oxygen of this ligand located in the same plane as the four peroxo oxygens. The H_2O ligand is situated *trans* to the oxo group, forming intermolecular hydrogen bonds with peroxo groups belonging to two adjacent complexes. Polynuclear molybdenum(VI) peroxo complexes containing amino acids, $[Mo_2O_4(O_2)_2L(H_2O)_4]$ (L = methionine, serine) and $[Mo_3O_7(O_2)_2L(H_2O)_6]$ (L = lysine, histidine), with bidentate organic ligand bonded to molybdenum oxo peroxo core, have been synthesized and spectroscopically characterized [13]. Recently dinuclear molybdenum(VI) peroxo complexes with aroyl hydrazones have been synthesized and characterized [14].

Metal complexes of Mannich bases have played a vital role in the development of coordination chemistry [15–17]. Studies on metal–peroxo complexes of formaldehyde-based Mannich bases have been reported [18]. Mononuclear oxodiperoxomolybdenum(VI) complexes, $[MoO(O_2)_2L\text{-}L]$ (where L-L = morpholinobenzyl benzamide, piperidinobenzyl benzamide, piperidinobenzyl urea, morpholinobenzyl urea, piperidinobenzyl thiourea, and morpholinobenzyl thiourea) have been thermally and spectroscopically studied [19]. In this work, we describe the synthesis and characterization of dinuclear molybdenum(VI) peroxo complexes with some benzaldehyde-based Mannich base ligands as continuation to our earlier work [19].

The structures of ligands are given in scheme 1.

2. Experimental

2.1. *Materials*

Ammonium heptamolybdate tetrahydrate (Merck), hydrogen peroxide (Merck), morpholine (Ranbaxy), piperidine (SDS), acetamide (Rankem), benzamide (Thomas Baker), benzaldehyde (Ranbaxy), 2-nitrobenzaldehyde (SRL), 3-nitrobenzaldehyde (SRL), and 4-nitrobenzaldehyde (Himedia) were used as supplied. Dimethyl sulfoxide (Ranbaxy) and ethanol (Commercial) were used after distillation. The ligands were prepared by the reported method [20, 21].

2.2. *Physical measurements and analytical methods*

Molar conductivity of complexes was measured at room temperature using 10^{-3} mol L^{-1} DMSO solution by Digital Conductivity Meter of type CC601 having a conductivity cell with a cell constant of 1.1. Magnetic measurements at room temperature were carried out by Gouy's method using $Hg[Co(NCS)_4]$ as standard. Melting points were determined on an Analab melting point apparatus and ^{1}H NMR spectra were obtained on a Bruker DPX 200 NMR spectrometer (200 MHz) in DMSO-d$_6$ using tetramethylsilane as an internal standard. Mass spectral data were obtained on ESI-esquires 3000 Bruker Daltonics spectrometer. IR spectra of complexes from 4000–400 cm^{-1} were recorded on Perkin-Elmer FT-IR spectrophotometer using KBr discs. Electronic spectra over the region 200–900 nm were recorded by UV-Vis single beam spectrophotometer Systronics using 10^{-3} mol L^{-1} DMSO solution of the complexes.

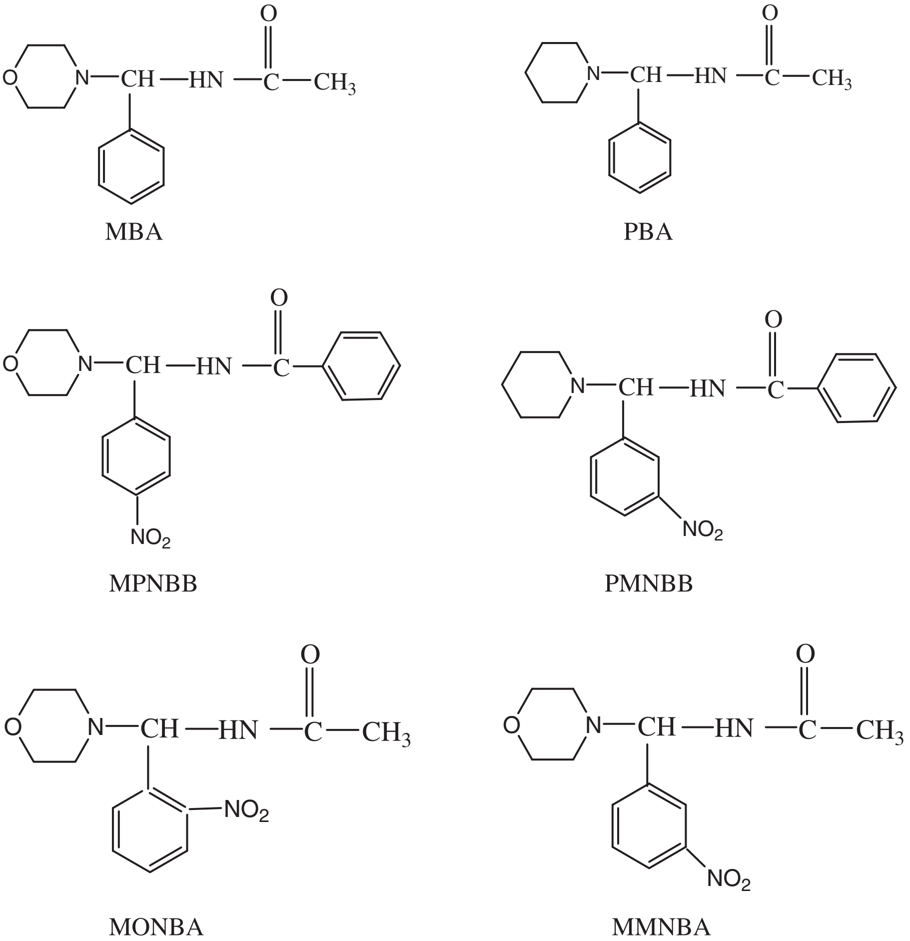

Scheme 1. Structures of ligands.

TGA/DTA studies were recorded on a Perkin-Elmer (Pyris Diamond) thermoanalyser at a heating rate of 10°C per minute in an atmosphere of nitrogen. Carbon, hydrogen, and nitrogen contents of the complexes were analyzed microanalytically using CHNS analyzer Leco Model-932. Molybdenum was determined gravimetrically as molybdenyl oxinate, $[MoO_2(C_9H_6ON)_2]$, after decomposing the complex with conc. nitric acid [22].

2.3. *Preparation of the complexes*

Ammonium heptamolybdate, $(NH_4)_6Mo_7O_{24} \cdot 4H_2O$ (1.235 g, 1 mmol) and H_2O_2 (30% w/v, 60 cm^3) were stirred for 6 h at 40°C. The light yellow solution obtained was filtered and to this filtrate ethanolic solution (20 cm^3) of ligand (1 mmol) was added; MBA (0.23 g), PBA (0.23 g), MPNBB (0.34 g), PMNBB (0.33 g), MONBA (0.27 g), and MMNBA (0.27 g). The resulting solution was again stirred for about 16 h at 40°C and then cooled overnight at room temperature. The precipitates formed in each case were filtered off, washed with aqueous ethanol and dried *in vacuo* at room temperature (yield, 62–84%).

3. Results and discussion

The analytical and spectroscopic results (tables 1–4) showed that all complexes are dinuclear with general formula, $[Mo_2O_4(O_2)_2L\text{-}L(H_2O)_2]\cdot H_2O$ (where L-L = MBA, PBA, MPNBB, PMNBB, MONBA, and MMNBA) having +6 oxidation state for Mo. All the complexes are white, stable at room temperature, insoluble in common organic solvents but fairly soluble in DMSO and DMF. The complexes do not have sharp melting points and decompose above 185°C.

3.1. *Conductance and magnetic measurements*

The molar conductivity values, λ_M of the complexes measured in $10^{-3}\,mol\,L^{-1}$ DMSO solution lie in the range $15\text{–}27\,Ohm^{-1}\,cm^2\,mol^{-1}$, which indicate the non-electrolytic nature of these complexes (table 1). Moreover, magnetic studies show that all the complexes are diamagnetic as expected for d^0 molybdenum(VI) complexes.

3.2. *IR spectral studies*

IR spectra of all the complexes (table 2) exhibit bands characteristic of the coordinated oxo, peroxo groups and the ligand molecule. All the complexes show three vibrational modes, 842–844, 651–669, and $606\text{–}618\,cm^{-1}$, assigned to ν(O–O), the asymmetric 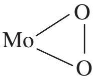 stretching (ν_{as}) and symmetric 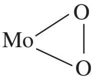 stretching (ν_s) modes, respectively. These bands confirm the η^2-coordination of the peroxo group [23]. The Mo–O–Mo vibration appears at $300\text{–}400\,cm^{-1}$, but is broad and poorly resolved [13]. An additional sharp band at $927\text{–}934\,cm^{-1}$ has been assigned to $\nu(Mo=O)$ [24, 25]. Thus, IR spectra confirm the presence of $[MoO(O_2)]^{2+}$ in these complexes.

In order to determine the mode of bonding of Mannich bases with molybdenum, the IR spectra of ligands were compared with those of corresponding complexes. In MBA and PBA ligands, sharp bands at 1648 and $1644\,cm^{-1}$ appeared due to $\nu(C=O)$ of amide group, respectively, and another band assigned to ν(C–N–C) of morpholine and piperidine rings appeared at 1136 and $1122\,cm^{-1}$, respectively (table 2). In the corresponding complexes, $[Mo_2O_4(O_2)_2MBA(H_2O)_2]\cdot H_2O$ and $[Mo_2O_4(O_2)_2PBA(H_2O)_2]\cdot H_2O$, these bands appear at lower frequencies at 1631, 1629, 1102, and $1102\,cm^{-1}$, respectively, indicating bonding of the ligands through carbonyl oxygen and ring nitrogen of morpholine/piperidine (table 2). Ring nitrogen of alicyclic amines in various ligands has been reported to coordinate [26].

In MPNBB and PMNBB, a sharp band due to $\nu(C=O)$ of amide group at 1640 and $1641\,cm^{-1}$, respectively, and another due to ν(C–N–C) of morpholine and piperidine rings at 1138 and $1140\,cm^{-1}$, respectively, shifted in $[Mo_2O_4(O_2)_2MPNBB(H_2O)_2]\cdot H_2O$

Table 1. Analytical data and some physical properties of peroxo complexes.

				Found (Calcd) %				
Complex	Empirical formula (Mol. wt.)	Color	Decomposition temperature (°C)	C	H	N	Mo	λ_M $(\mathrm{Ohm}^{-1}\,\mathrm{cm}^{-2}\,\mathrm{mol}^{-1})$
$[Mo_2O_4(O_2)_2MBA(H_2O)_2]\cdot H_2O$	$Mo_2C_{13}H_{24}N_2O_{13}$ (608.21)	White	200	25.58 (25.67)	3.72 (3.97)	4.52 (4.60)	31.50 (31.54)	19
$[Mo_2O_4(O_2)_2PBA(H_2O)_2]\cdot H_2O$	$Mo_2C_{14}H_{26}N_2O_{12}$ (606.24)	White	212	27.70 (27.73)	4.19 (4.32)	4.54 (4.62)	31.62 (31.65)	15
$[Mo_2O_4(O_2)_2MPNBB(H_2O)_2]\cdot H_2O$	$Mo_2C_{18}H_{25}N_3O_{15}$ (715.28)	White	222	30.12 (30.22)	3.44 (3.52)	3.73 (3.91)	26.80 (26.82)	22
$[Mo_2O_4(O_2)_2PMNBB(H_2O)_2]\cdot H_2O$	$Mo_2C_{19}H_{27}N_3O_{14}$ (713.31)	White	185	31.85 (31.99)	3.65 (3.81)	5.82 (5.89)	26.83 (26.89)	27
$[Mo_2O_4(O_2)_2MONBA(H_2O)_2]\cdot H_2O$	$Mo_2C_{13}H_{23}N_3O_{15}$ (653.21)	White	198	23.73 (23.90)	3.49 (3.54)	6.32 (6.43)	29.31 (29.37)	24
$[Mo_2O_4(O_2)_2MMNBA(H_2O)_2]\cdot H_2O$	$Mo_2C_{13}H_{23}N_3O_{15}$ (653.21)	White	190	23.81 (23.90)	3.45 (3.54)	6.36 (6.43)	29.30 (29.37)	20

Table 2. IR spectral data (cm^{-1}) of peroxo complexes.

Ligand	$\nu(C=O)$	$\nu(C–N–C)$	Complex	$\nu(Mo=O)$	$\nu(C=O)$	$\nu(C–N–C)$	$\nu(O–O)$	$\nu_{as}\left(\mathrm{Mo}\begin{smallmatrix}\diagup\,\mathrm{O}\\ \,\vert\\ \diagdown\,\mathrm{O}\end{smallmatrix}\right)$	$\nu_{s}\left(\mathrm{Mo}\begin{smallmatrix}\diagup\,\mathrm{O}\\ \,\vert\\ \diagdown\,\mathrm{O}\end{smallmatrix}\right)$	$\nu(OH)$
MBA	1648	1136	$[Mo_2O_4(O_2)_2MBA(H_2O)_2]\cdot H_2O$	928	1631	1102	843	651	606	3436
PBA	1644	1122	$[Mo_2O_4(O_2)_2PBA(H_2O)_2]\cdot H_2O$	928	1629	1102	843	651	606	3429
MPNBB	1640	1138	$[Mo_2O_4(O_2)_2MPNBB(H_2O)_2]\cdot H_2O$	928	1631	1102	843	652	606	3422
PMNBB	1641	1140	$[Mo_2O_4(O_2)_2PMNBB(H_2O)_2]\cdot H_2O$	934	1631	1113	844	669	618	3427
MONBA	1650	1142	$[Mo_2O_4(O_2)_2MONBA(H_2O)_2]\cdot H_2O$	927	1631	1102	842	651	611	3436
MMNBA	1649	1140	$[Mo_2O_4(O_2)_2MMNBA(H_2O)_2]\cdot H_2O$	928	1631	1102	843	651	606	3438

Table 3. Electronic spectral data (nm) of peroxo complexes.

Complex	$\pi O_2^{2-} \rightarrow dMo$	$O^{2-} \rightarrow dMo$
$[Mo_2O_4(O_2)_2MBA(H_2O)_2] \cdot H_2O$	350	278
$[Mo_2O_4(O_2)_2PBA(H_2O)_2] \cdot H_2O$	341	274
$[Mo_2O_4(O_2)_2MPNBB(H_2O)_2] \cdot H_2O$	336	274
$[Mo_2O_4(O_2)_2PMNBB(H_2O)_2] \cdot H_2O$	348	287
$[Mo_2O_4(O_2)_2MONBA(H_2O)_2] \cdot H_2O$	349	265
$[Mo_2O_4(O_2)_2MMNBA(H_2O)_2] \cdot H_2O$	338	274

and $[Mo_2O_4(O_2)_2PMNBB(H_2O)_2] \cdot H_2O$, $\nu(C=O)$ to 1631 cm^{-1} and ν(C–N–C) of morpholine and piperidine to 1102 and 1113 cm^{-1}, respectively. Both bands exhibit negative shifts relative to their corresponding positions in free states, indicating coordination through carbonyl oxygen and ring nitrogen.

In MONBA, $\nu(C=O)$ appeared at 1650 cm^{-1} and ν(C–N–C) of morpholine at 1142 cm^{-1}, whereas in MMNBA, $\nu(C=O)$ appeared at 1649 cm^{-1} and ν(C–N–C) of morpholine at 1140 cm^{-1}. In both complexes, $[Mo_2O_4(O_2)_2MONBA(H_2O)_2] \cdot H_2O$ and $[Mo_2O_4(O_2)_2MMNBA(H_2O)_2] \cdot H_2O$, $\nu(C=O)$ appeared at 1631 cm^{-1} and ν(C–N–C) of morpholine appeared at 1102 cm^{-1}. As compared to free ligands, both bands show negative shifts, indicating coordination of molybdenum through carbonyl oxygen and ring nitrogen.

3.3. *Electronic spectral studies*

Electronic spectra of these complexes recorded in 10^{-3} mol L^{-1} DMSO (table 3) show two high energy absorption bands at 274–350 nm. The bands are close in energy and cannot be assigned precisely. However, they may be assigned to peroxo → molybdenum and oxygen (π and σ) → molybdenum charge transfer (LMCT) bands [27]. The molar extinction coefficients of these bands lie in the range 3000–3670 L cm^{-1} mol^{-1}. There was no evidence of any d–d transition. This result is consistent with the presence of Mo(VI) system in the complexes.

3.4. *^{1}H NMR studies*

The ^{1}H NMR spectrum of N-[1-morpholino(-4-nitrobenzyl)] benzamide (MPNBB) was recorded in deuterated methanol (figure 1 in Supplementary material), showing a triplet at δ 2.79 for N-CH$_2$ of morpholine ring and a triplet at δ 4.10 for O–CH$_2$ of morpholine ring. The aromatic protons of phenyl ring in O_2N–Ph–CH ortho to –CH group appear as a doublet of doublets at δ 7.62, whereas the aromatic protons of the same phenyl ring meta to –CH group appear as a doublet at δ 8.23. In $[Mo_2O_4(O_2)_2MPNBB(H_2O)_2] \cdot H_2O$, the peaks corresponding to four protons of –CH$_2$ groups of N–CH$_2$ in the morpholine ring undergo downfield shift to δ 2.99, due to coordination of ring nitrogen of morpholine with molybdenum (figure 2 in Supplementary material).

Table 4. Mass spectral data of $[Mo_2O_4(O_2)_2MBA(H_2O)_2] \cdot H_2O$ with relative isotopic abundances of its fragment ions formed.

Complex $Mo_2O_4(O_2)_2$ $MBA(H_2O)_2 \cdot H_2O$	*m/z* (%)	M − 8* %	M − 6* %	M − 5* %	M − 4* %	M − 3* %	M − 2* %	M − 1* %	M* %	M + 1* %	M + 2* %	M + 3* %	M + 4* %	M + 5* %	M + 6* %	M + 8* %
$[Mo_2O_4(O_2)_2$ $MBA(H_2O)_2 \cdot H_2O]^+$	608 (21.87)	14.9	19.1	35.0	45.0	46.6	94.3	63.0	100	89.7	87.9	66.5	72.5	24.3	36.0	7.6
$[Mo_2O_4(O_2)_2MBA]^+$	554 (84.37)	15.0	19.2	35.2	45.1	46.6	94.6	63.0	100	89.8	87.7	66.3	72.3	24.0	35.8	7.4
$[MoO(O_2)_2MBA]^+$	412 (84.37)		57.0		36.9	66.7	74.3	48.0	100	15.2	39.4					
$[Ph\text{-}CH\text{-}NH\text{-}CO]^+$	133 (100)								100	9.1						

MBA = 234.29; * = relative isotopic abundances; % = relative peak intensity; *m/z* is calculated using Mo mass equal to 98 amu and Mo_2 mass equal to 192 amu.

3.5. *Thermal studies*

The TG curve of a representative complex $[Mo_2O_4(O_2)_2MBA(H_2O)_2] \cdot H_2O$ (figure 3 in "Supplementary material") shows initially a weight loss of 2.73% starting from 22 to 112°C corresponding to the loss of outer sphere water molecule (calculated weight loss = 2.95%). This is supported by appearance of an endothermic peak in the DTA curve at 51.36°C. Further heating up to 450°C shows weight loss of 16.29% attributable to loss of two peroxo groups and two coordinated water molecules (calculated weight loss = 16.44%) leading to the probable formation of the decomposition product. Mo_2O_4MBA, which is stable up to 750°C. The IR spectrum of this intermediate showed absence of peaks due to peroxo. The DTA curve shows a sharp exothermic peak at 282.50°C corresponding to loss of dioxygen, followed by an endothermic peak at 360.65°C, which is due to loss of coordinated water molecules.

$$\left[Mo_2O_4(O_2)_2MBA(H_2O)_2\right] \cdot H_2O \rightarrow Mo_2O_4(O_2)_2MBA(H_2O)_2 + H_2O, \tag{1}$$

$$Mo_2O_4(O_2)_2MBA(H_2O)_2 \rightarrow Mo_2O_4MBA + 2O_2 + 2H_2O. \tag{2}$$

On heating above 750°C, the intermediate undergoes weight loss of 36.99% corresponding to loss of MBA (calculated weight loss = 38.52%). Thereafter, no further weight loss takes place after 850°C, leading to the formation of $2MoO_2$ as end product.

$$Mo_2O_4MBA \rightarrow 2MoO_2 + MBA. \tag{3}$$

3.6. *ESI mass spectral studies*

The ESI mass spectrum of the representative complex $[Mo_2O_4(O_2)_2MBA(H_2O)_2] \cdot H_2O$ shows the molecular ion peak at m/z 608 (M^+) and the base peak at m/z 133, which is due to the organic fragment, $[Ph–CH–NH–CO]^+$. Two other significant peaks appear in the mass spectrum of the complex, one at m/z 554, corresponding to $[Mo_2O_4(O_2)_2MBA]^+$, and the other at m/z 412, corresponding to the mononuclear oxodiperoxo fragment, $[MoO(O_2)_2MBA]^+$. The intensities of all peaks have been represented relative to base peak at m/z 133 (table 4). Masses of the fragment ions listed in the table are calculated using one molybdenum atom mass equal to 98 amu and the total mass of two molybdenums equal to 192 amu as these are the most abundant isotopes which appear in the isotope pattern of Mo and Mo_2 units, respectively.

Mo has seven isotopes with atomic masses of 92, 94, 95, 96, 97, 98, and 100 whereas Mo_2 moiety has 15 isotopes with atomic masses of 184, 186, 187, 188, 189, 190, 191, 192, 193, 194, 195, 196, 197, 198, and 200. The overlap of these isotope patterns occurs in the mass spectrum [28]. Further the molecular ion is a dimolybdenum fragment, so around the molecular ion peak at m/z 608, an isotopic envelope of 15 different peaks, with distinctive ratios one to another, spanning 16 mass units is observed [28]. The most intense isotope peak (in this fragment ion at m/z 608) is set to 100% and percentages of the other isotope peaks are computed relative to it (table 4). Also the dimolybdenum fragment, $[Mo_2O_4(O_2)_2MBA]^+$, shows the similar isotopic pattern of 15 different peaks. The monomolybdenum fragment ion, $[MoO(O_2)_2MBA]^+$, shows an isotopic

Table 5. Antibacterial activity data of the ligands and their complexes against *Ralastonia solanacearum*.

	Diameter of the inhibition zone (mm) at different concentrations		
Complex	500 ppm	1000 ppm	2000 ppm
MBA (1)	5	8	17
PBA (2)	4.5	7.5	16
$[Mo_2O_4(O_2)_2MBA(H_2O)_2] \cdot H_2O$ (3)	9	18	34
$[Mo_2O_4(O_2)_2PBA(H_2O)_2] \cdot H_2O$ (4)	8.5	19	40
Water (Control)	0	0	0

envelope spanning only eight mass units. Here, the most intense isotope peak (at m/z 412) is set to 100% and percentages of the other isotope peaks are computed relative to it (table 4). The observed and theoretical isotopic distribution of the fragment ion $[Mo_2O_4(O_2)_2MBA(H_2O)_2 \cdot H_2O]^+$ is shown in figure 4 in "Supplementary material".

3.7. *Antibacterial activity*

The *in vitro* biological screening effects of the ligands and the corresponding complexes were tested against standard strains of the bacterium *Ralastonia solanacearum* (*Pseudomonas solanacearum*) causing bacterial wilt in solanaceous vegetables. The paper disc plate method (disc diffusion method) [29, 30] described by Skinner was employed to evaluate bactericidal activity. In this method, sterilized nutrient agar culture medium was first prepared [30] and then transferred to previously washed and sterilized petriplates. The plates were frozen at about 40°C for inoculation. Bacterial strains were then applied on the solid culture medium with the help of a platinum wire loop. The test solutions were prepared by dissolving the ligands in ethanol and the complexes in DMSO. The concentrations used in this study were 500, 1000, and 2000 ppm. Water of corresponding concentration was used as control. In a typical procedure, filter paper discs of 5 mm diameter and 1 mm thickness were dipped into the test solution of each compound separately for 2 h. These discs were then applied on the previously inoculated (seeded) agar plates using sterilized forceps and incubated at 25°C for 48 h. During this period, the test solution diffused and the growth of the inoculated organism was affected. The activity of the compounds was estimated by measuring the diameter of the inhibition zone (clear area around the disc) developed on each plate in millimeter (figure 5 in Supplementary material). Blank tests showed that ethanol and DMSO used in the preparation of the test solutions does not affect the test organism. Each treatment was repeated three times to minimize error and average data were taken as the final result. The work was carried out under aseptic conditions.

Table 5 shows that on increasing the concentration of the complexes, the diameter of the inhibition zone also increases that is, the compounds showed higher activity with increase in concentration in the test range. Again, it is evident from the antibacterial screening data (table 5) that the metal complexes are more potent than the parent ligands. The chelation theory accounts for the increased activity of the metal complexes [31]. Apart from this, other factors such as solubility, conductivity, and dipole moment (influenced by the presence of metal ions) also may be possible reasons for increasing this activity [30].

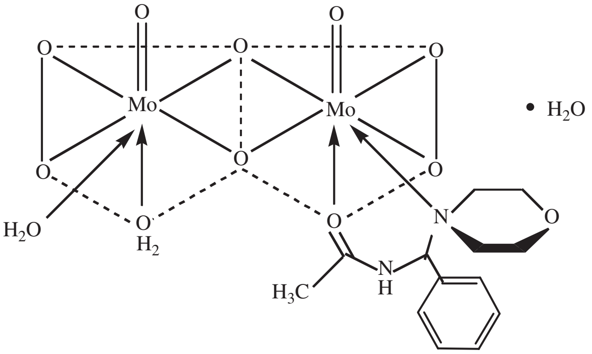

Scheme 2. Structure of $[Mo_2O_4(O_2)_2MBA(H_2O)_2] \cdot H_2O$.

4. Conclusion

From the physico-chemical and spectral evidence discussed above, we conclude that all the complexes are dimeric with composition, $[Mo_2O_4(O_2)_2L\text{-}L(H_2O)_2] \cdot H_2O$ [where L-L = MBA, PBA, MPNBB, PMNBB, MONBA, and MMNBA] having +6 oxidation state for Mo. Further, we propose that in these dinuclear complexes, each molybdenum is seven-coordinate with pentagonal bipyramidal geometry. The proposed structure for $[Mo_2O_4(O_2)_2MBA(H_2O)_2] \cdot H_2O$ is given as scheme 2. Both the peroxo groups are bound sideways, one to each molybdenum, and the metal centers are connected through oxygen bridges.

Acknowledgments

We are grateful to the Head, Pathology Division, SKAUST, Jammu for antibacterial studies. We also wish to thank the Head, Department of Physics, University of Jammu for TGA and Director, IIIM for library and spectral studies.

References

[1] B.C. Gates, J.R. Katzen, A. Schuit. *Chemistry of Catalytic Processes*, p. 390, McGraw-Hill, New York, (1979); S.K. Das, D. Biswas, Chaudhury, S. Sarkar. *J. Am. Chem. Soc.*, **116**, 9061 (1994).
[2] M.L.H. Green. *Proceedings of 3rd International Conference on Chemistry and Uses of Molybdenum*, H.F. Barry, P.C.H. Mitchel. (Eds), p. 34, Climax Molybdenum Co., Ann Arbor, MI, (1979).
[3] F.R. Sensato, Q.B. Cass, E. Longo, J.Z. Schpector, R. Custodio, J. Andres, M.Z. Hernandes, R.L. Longo. *Inorg. Chem.*, **40**, 6022 (2001).
[4] S. Das, T. Bhowmick, T. Pumniyamurthy, D. Dey, J. Nath, M.K. Chaudhuri. *Tetrahedron Lett.*, **44**, 4915 (2003).
[5] E.I. Stiefel. *Prog. Inorg. Chem.*, **2**, 1 (1977), and references therein.
[6] J.A. Connor, E.A.V. Ebsworth. *Adv. Inorg. Chem. Radiochem.*, **6**, 279 (1964).
[7] E.I. Stiefel. *Prog. Inorg. Chem.*, **22**, 1 (1977).
[8] M.H. Dickman, M.T. Pope. *Chem. Rev.*, **94**, 569 (1994).
[9] R. Stomberg. *Acta Chem. Scand.*, **24**, 1072 (1968).

[10] W. Shum. *Inorg. Chem.*, **25**, 4324 (1986).

[11] M.C. Chakraborti, S. Ganguly, M. Bhattacharjee. *Polyhedron*, **12**, 55 (1993).

[12] V. Nardello, J. Marko, G. Vermeersch, J.M. Aubry. *Inorg. Chem.*, **34**, 1950 (1995).

[13] K. Serdiuk, R. Gancarz, M.C. Golonka. *Transition Met. Chem.*, **26**, 538 (2001).

[14] M. Saleem, M. Sharma, H.N. Sheikh, B.L. Kalsotra. *Indian J. Chem.*, **46 A**, 1423 (2007).

[15] N. Raman, S. Ravichandran. *Polish J. Chem.*, **78**, 2005 (2004).

[16] R.C. Paul, P.A. Kapila, S. Bedi, K.K. Vasisht. *J. Indian Chem. Soc.*, **53**, 768 (1976).

[17] N. Raman, S. Ravichandran. *Asian J. Chem.*, **15**, 1848 (2003).

[18] A. Sabastiyan, D. Venkappayya. *J. Indian Chem. Soc.*, **67**, 584 (1990).

[19] M. Sharma, M. Saleem, M.S. Pathania, H.N. Sheikh, B.L. Kalsotra. *Chin. J. Chem.*, **27**, 1 (2009).

[20] G. Venkatesa Prabhu, D. Venkappayya. *J. Indian Chem. Soc.*, **72**, 511 (1995).

[21] N. Raman, R. Vimalaramani, C. Thangaraja. *Indian J. Chem.*, **43 A**, 2357 (2004).

[22] A.I. Vogel. *A Text Book of Quantitative Inorganic Analysis*, 3rd Edn, Longmans and Green Co. Ltd, London (1968).

[23] C. Djordjevic, N. Vuletic, B.A. Jacobs, E. Sin. *Inorg. Chem.*, **36**, 1798 (1997).

[24] M.K. Chaudhuri, B. Das. *Inorg. Chem.*, **25**, 168 (1986).

[25] M.S. Reynolds, A. Buttler. *Inorg. Chem.*, **35**, 2378 (1996).

[26] H.N. Sheikh, A. Hussain, B.L. Kalsotra. *Russ. J. Inorg. Chem.*, **51**, 724 (2006).

[27] I.S. Ahuja, A. Garg. *Inorg. Nucl. Chem. Lett.*, **7**, 937 (1971).

[28] E. Hochberg, P. Walks, E.H. Abbott. *Inorg. Chem.*, **13**, 1824 (1974).

[29] M.S. Rahman, M.N. Anwar. *Bangladesh J. Microbiol.*, **24**, 73 (2007) and references therein.

[30] Z.H. Chohan, M.A. Farooq. *Synth. React. Inorg. Met.-Org. Chem.*, **31**, 1853 (2001) and references therein.

[31] R.V. Singh, R. Dwivedi, S.C. Joshi. *Transition Met. Chem.*, **29**, 70 (2004).